



HAL
open science

Investigating uncertainties in zooplankton composition shifts under climate change scenarios in the Mediterranean Sea

Fabio Benedetti, François Guilhaumon, Fanny Adloff, Sakina-Dorothee Ayata

► **To cite this version:**

Fabio Benedetti, François Guilhaumon, Fanny Adloff, Sakina-Dorothee Ayata. Investigating uncertainties in zooplankton composition shifts under climate change scenarios in the Mediterranean Sea. *Ecography*, 2017, 10.1111/ecog.02434 . hal-01495992

HAL Id: hal-01495992

<https://hal.sorbonne-universite.fr/hal-01495992v1>

Submitted on 27 Mar 2017

HAL is a multi-disciplinary open access archive for the deposit and dissemination of scientific research documents, whether they are published or not. The documents may come from teaching and research institutions in France or abroad, or from public or private research centers.

L'archive ouverte pluridisciplinaire **HAL**, est destinée au dépôt et à la diffusion de documents scientifiques de niveau recherche, publiés ou non, émanant des établissements d'enseignement et de recherche français ou étrangers, des laboratoires publics ou privés.

1 *Manuscript under revision for Ecography*

2
3 **Title: Investigating uncertainties in zooplankton composition shifts**
4 **under climate change scenarios in the Mediterranean Sea**

5
6 Authors: Fabio Benedetti¹, François Guilhaumon², Fanny Adloff³, Sakina-Dorothee
7 Ayata¹

8 Affiliations:

9 1) Sorbonne Universités, UPMC Université Paris 06, CNRS, Laboratoire
10 d’océanographie de Villefranche (LOV), Observatoire Océanologique, 06230
11 Villefranche-sur-Mer, France.

12 2) IRD UMR 9190 MARBEC, IRD-CNRS-IFREMER-UM, Université de Montpellier,
13 Montpellier 34095, France.

14 3) CNRM UMR 3589, Météo-France/CNRS, Toulouse, France

15
16 **Abstract**

17 Ensemble niche modelling has become a common framework to predict changes in
18 assemblages composition under climate change scenarios. The amount of
19 uncertainty generated by the different components of this framework has rarely been
20 assessed. In the marine realm forecasts have usually focused on taxa representing
21 the top of the marine food-web, thus overlooking their basal component: the
22 plankton. Calibrating environmental niche models at the global scale, we modelled
23 the habitat suitability of 106 copepod species and estimated the dissimilarity between
24 present and future zooplanktonic assemblages in the surface Mediterranean Sea.
25 We identified the patterns (species replacement *versus* nestedness) driving the
26 predicted dissimilarity, and quantified the relative contributions of different uncertainty
27 sources: environmental niche models, greenhouse gas emission scenarios,
28 circulation model configurations, and species prevalence. Our results confirm that the
29 choice of the niche modelling method is the greatest source of uncertainty in habitat
30 suitability projections. Presence-only and presence-absence methods provided
31 different visions of the niches, which subsequently lead to different future scenarios
32 of biodiversity changes. Nestedness with decline in species richness is the pattern
33 driving dissimilarity between present and future copepod assemblages. Our
34 projections contrast with those reported for higher trophic levels, suggesting that
35 different components of the pelagic food-web may respond discordantly to future
36 climatic changes.

37
38 **Introduction**

39 The last decade witnessed the emergence of environmental niche models as a
40 popular tool for studying biogeography and macroecology (Zimmermann et al. 2010;
41 Brotons 2014). Environmental Niche Models (ENMs) refer to a wide array of
42 statistical methods that enable scientists to empirically relate the distribution of a
43 species to a suite of abiotic predictors in order to approximate its environmental niche
44 (*sensu* Hutchinson 1957). The constructed models can be used to infer areas of
45 potential habitat suitability for the species within, or outside, its known spatial range
46 (Guisan and Zimmermann 2000; Owens et al. 2012). In a context of climate change,
47 ENMs have been increasingly coupled with climate models to forecast future
48 changes in species habitat suitability and distributions (Pearson and Dawson 2003;
49 Guisan and Thuiller 2005; Brotons 2014). ENMs can be used to identify regions with

50 potential diversity losses or gains, and can therefore help in determining priority
51 areas for biodiversity management (Bellard et al. 2012).

52 The niche modelling procedure is sprinkled with decisional steps, from the initial
53 conditions to the projections. Each step requires a decision among alternative
54 options, and each option has a consequence on the final inference, thus generating
55 variability (or uncertainty) around the mean projection (Araújo and New 2007;
56 Beaumont et al. 2008). Uncertainty maps are often not provided with ENMs
57 predictions (Rocchini et al. 2011). Studies quantifying and mapping uncertainties
58 associated with niche models predictions are scarce and are generally based on
59 terrestrial taxa such as New World birds (Diniz-Filho et al. 2009), freshwater fishes in
60 France (Buisson et al. 2010), African vertebrates (Garcia et al. 2012), and European
61 trees (Goberville et al. 2015). While these studies have identified the choice of the
62 statistical technique to be the main driver of uncertainty, there is still no consensus
63 on the best model. Ensemble forecasting has therefore been suggested as a solution
64 to handle the variability of predictions based on different methods (Araújo and New
65 2007). But distinct modelling strategies often rely on different theoretical assumptions
66 and data properties (e.g. presence-only *versus* presence-absence data, or distance-
67 based *versus* regression-based methods), and therefore may not approximate the
68 same facet of a species niche (Soberón and Nakamura 2009; Sillero 2011).
69 Consequently, more research is needed to summarise the relative importance of the
70 different choices made within the niche modelling framework (i.e. aims of the study,
71 species' ecological properties, ENM type and complexity, data characteristics etc.).

72 Oceans play a key role in regulating Earth's climate (Sabine et al. 2004) and provide
73 energetic and food resources for people throughout the world. Since climate change
74 is threatening marine biodiversity and the associated ecosystem services (Hoegh-
75 Guldberg and Bruno 2010; Gattuso et al. 2015), it is crucial to better understand how
76 species may respond to environmental fluctuations and how the later may impact
77 ecosystem functioning. Additionally, marine taxa live in habitats with different
78 characteristics compared to their terrestrial peers: there are fewer barriers to
79 dispersal (Steele 1991), and temperature gradients are declined over much larger
80 spatial scales. Moreover, marine taxa present original life cycles and ecological
81 characteristics (ontogenetic shifts, spatial aggregation, mobility), as well as peculiar
82 data properties (and biases) which may pose new challenges for niche modelling
83 (Robinson et al. 2011). Occurrence-based niche modelling has been relatively
84 ignored in marine ecology (Robinson et al. 2011). Rather, marine ecologists have
85 focused on the available abundance records to model the population dynamics of
86 high trophic level taxa and their impact on food supplies (Cheung et al. 2010), or to
87 relate their distribution shifts to climate fluctuations (Perry et al. 2005; Pinsky et al.
88 2013).

89 Amid all oceanic basins, the Mediterranean Sea occupies a particular position: this
90 semi-enclosed basin is a hotspot for biodiversity (Myers et al. 2000; Bianchi and
91 Morri 2000) that undergoes intense human pressures (The MerMex Group 2011; Coll
92 et al. 2012) and strong rates of warming due to anthropogenic climate change (Giorgi
93 2006). Ongoing and future warming of the basin will likely trigger biodiversity losses
94 across different benthic communities (Danovaro et al. 2004; Garrabou et al. 2009;
95 Coma et al. 2009). Pelagic communities are also likely to experience alterations in
96 species composition due to the northwards migrations of species tracking their
97 optimal thermal niche (Sabatès et al. 2006). Northwards migration would promote the
98 replacement of cold-water species by warm-water competitors (Ben Rais Lasram et
99 al. 2010; Albouy et al. 2012), thus leading to alterations in the food-web structure and

100 modifications of the functional and phylogenetic components of biodiversity (Albouy
101 et al. 2014, 2015). However, previous projections only concerned coastal fish
102 assemblages. Potential community shifts in the lower trophic levels (i.e. the plankton)
103 are still lacking despite their major ecological importance. Mediterranean fishes
104 primarily feed on mesozooplankton (Stergiou and Karpouzi 2002; Costalago et al.
105 2014), a group that is dominated (in terms of abundance and diversity) by copepods
106 (Siokou-Frangou et al. 2010; Mazzocchi et al. 2014). Copepods represent a key
107 group in pelagic trophic webs and are major contributors to the marine carbon cycle
108 (Mauchline 1998; Beaugrand et al. 2010). Climate variability has been shown to
109 modify copepod biogeography and phenology (Beaugrand et al. 2002; Mackas et al.
110 2012), therefore altering upper trophic levels through bottom-up processes
111 (Beaugrand and Kirby 2010). Copepods have been identified as “beacons of climate
112 change” (Richardson 2008) meaning they are an ideal group for monitoring changes
113 in environmental conditions, and the ensuing ecosystem modifications. For these
114 reasons, ENMs are appropriate and necessary tools to estimate climate change
115 impacts on copepod assemblages (Sunday et al. 2012).

116 Plankton belong to the taxa that are the least studied through occurrence-based
117 niche modelling (Robinson et al. 2011). To our knowledge, only four studies have
118 used ENMs to model species niches for oceanic phytoplankton (Irwin et al. 2012;
119 Pinkernell and Beszteri 2014; Brun et al. 2015; Barton et al. 2016). Zooplankton has
120 been subjected to more niche-based studies, yet nearly all ENMs were developed for
121 the North Atlantic and they implied a limited set of model algorithms and species
122 (Reygondeau and Beaugrand 2011; Beaugrand et al. 2013; Chust et al. 2013;
123 Villarino et al. 2015; Brun et al. 2016). These studies have focused on predicting
124 shifts in habitat suitability for a few species and on inferring changes in local
125 biodiversity (α diversity). To account for changes in species assemblages
126 composition, one can use indices of β diversity (representing the variation of species
127 assemblages composition; Anderson et al. 2011), and combine them with α diversity
128 estimates to identify the patterns driving dissimilarity between present and future
129 species assemblages (Dobrovolski et al. 2012).

130 The aims of our study are to: (i) estimate potential shifts in zooplankton surface
131 assemblages composition in the Mediterranean Sea under several climate change
132 scenarios; and (ii) quantify the relative importance of uncertainty sources. Shifts in
133 assemblages composition are derived from a set of ten ENMs, covering the majority
134 of the commonly-used algorithms, and six different configurations of a regional
135 circulation model. These configurations allow investigating the effects of greenhouse
136 gas (GHG) emission scenarios and boundary forcings (BF), the consequences of the
137 latter having never been explored before though it has been shown to be at least of
138 the same order of magnitude as the one related to the GHG emission scenario
139 (Adloff et al. 2015). In addition, five different levels in species prevalences are tested
140 to investigate this potential source of substantial uncertainty (see below).

141

142 **Material and Methods**

143 *Species data*

144 To select the copepod species to be modelled, we filtered those with more than 50
145 occurrences in the Mediterranean Sea, based on a regional dataset (Supplementary
146 material Appendix 1, Table A1) and, since these are not endemic, we selected only
147 those represented globally in the Ocean Biogeographic Information System (OBIS;
148 <http://www.iobis.org>), which lead to a total of 106 copepod species. Models were
149 therefore calibrated using global data to avoid truncated distributions (Thuiller et al.

150 2004). The species list represents nearly 20% of the total number of copepod
151 species reported in the Mediterranean Sea ($n = 560$, Razouls et al. 2005-2016). Most
152 of the missing species being rare, our species list does represent the most commonly
153 sampled species in the basin (Siokou-Frangou et al. 2010, Mazzocchi et al. 2014).
154 Observations were aggregated within the $0.25^\circ \times 0.25^\circ$ grid cells of the World Ocean
155 Atlas 2013 (WOA13; Levitus et al. 2013). Ultimately, only the presences recorded
156 across a defined 30-year baseline period (1965-1994) were kept. See Supplementary
157 material Appendix 2, Table A2, for the final list of copepod species names and their
158 corresponding numbers of global and regional occurrences after re-sampling on
159 WOA13's grid.

160

161 *Present and future climatic data*

162 Sea surface temperature (SST) and sea surface salinity (SSS) were used as
163 environmental predictors. These variables are commonly used when modelling
164 copepod distributions because copepods are: poikilothermic, passively dispersed,
165 and not exploited by human activities (Richardson 2008; Reygondeau and
166 Beaugrand 2011; Chust et al. 2013).

167 Since the use of 30-year climatologies is often advocated for calibrating ENMs when
168 predicting species distributions under climate change scenarios (Roubicek et al.
169 2010; Harris et al. 2014), 30-year climatologies for the baseline period (1965-1994)
170 were constructed as follows. First, four global seasonal (spring/summer/fall/winter)
171 SST and SSS *in situ* climatologies were retrieved from the WOA13 (Locarnini et al.
172 2013; Zweng et al. 2013; available at: [https://www.nodc.noaa.gov/cgi-](https://www.nodc.noaa.gov/cgi-bin/OC5/woa13/woa13.pl)
173 [bin/OC5/woa13/woa13.pl](https://www.nodc.noaa.gov/cgi-bin/OC5/woa13/woa13.pl)) at a $1/4^\circ$ resolution, for each of the three decades
174 constituting the chosen baseline periods: 1965-1974, 1975-1984, 1985-1994. For
175 each variable, global decadal climatologies were computed by averaging the four
176 initial seasonal climatologies. In addition, the standard deviation of SST was
177 computed to obtain decadal climatologies of the seasonal variation of SST (σ SST) for
178 each of the three periods. The newly-defined decadal climatologies were used to
179 compute the final estimates of average SST, average SSS, and average σ SST for
180 the 1965-1994 period, which were used to calibrate the ENMs.

181 Future predictions of SST, SSS and σ SST over the Mediterranean Sea were
182 obtained from the regional ocean general circulation model NEMOMED8 (Beuquier et
183 al. 2010) under multiple forcing configurations (Adloff et al. 2015). Its horizontal
184 resolution is $1/8^\circ$ (~9 to 12 km grid cells depending on latitude) and it has 43 vertical
185 levels. NEMOMED8 has been previously used to project fish distributions under
186 climate change scenarios (Ben Rais Lasram et al. 2010; Albouy et al. 2012; Hattab et
187 al. 2014).

188 This ocean model presents three main sources of boundary forcing: the Atlantic
189 hydrography, the river runoff and the atmospheric surface fluxes. To assess
190 projection uncertainty related to the choice of the GHG emission scenario and to the
191 choice of the different boundary forcings, we used the 6-member ensemble scenario
192 simulations of Adloff et al. (2015). In their numerical experiments, the origin of the
193 model boundary forcings (surface flux, river runoff, and Atlantic hydrography) was
194 alternatively changed, and three different scenarios of GHG emission were
195 considered. The GHG emission scenarios used in their study are based on the
196 Special Report on Emission Scenarios (SRES) of the Intergovernmental Panel for
197 Climate Change (IPCC 2007). The authors' annotations for the model runs were kept
198 (A2, A2-F, A2-RF, A2-ARF, A1B-ARF, B1-ARF) with A2, A1B, and B1 indicating the
199 GHG emission scenario, F the updated surface fluxes conditions, R the updated river

200 runoff conditions, and A the updated Atlantic hydrography conditions. The sensitivity
201 to each of the ocean model boundary forcings can be assessed through the “one to
202 one” comparison among the simulations A2, A2-F, A2-RF, and A2-ARF. The
203 comparison between A2-ARF, A1B-ARF, and B1-ARF allows to assess the
204 uncertainty related to the choice of the GHG emission scenario. The latest IPCC
205 report provides more recent GHG concentration scenarios (Representative
206 Concentration Pathways RCPs; IPCC 2013), but to date there is no regionalized
207 climate change model for the Mediterranean Sea under RCP scenarios.

208 Monthly outputs of the ocean model were used to calculate seasonal and decadal
209 climatologies of mean SST, mean SSS, and mean σ SST following the WOA13 mode
210 (Levitus et al. 2013) for two future 30-year periods: 2020-2049 and 2069-2098.
211 Similarly, monthly outputs for the baseline period were used to construct additional
212 climatologies of mean SST, SSS and σ SST. These were used to compute the
213 modelled climatological anomalies for the three environmental predictors. The
214 modelled climatological anomalies were added to the baseline in situ climatologies to
215 obtain future fields of SST, SSS, and σ SST that are corrected for the bias between
216 NEMOMED8 outputs and the observations. Therefore, the ENMs that were calibrated
217 on observational climatologies were not directly projected on modelled data (Hattab
218 et al. 2014).

219 The final climatologies were then used to project the habitat suitabilities of the 106
220 species in 2020-2049 and 2069-2098 using the ENMs (Fig. 1). See Supplementary
221 material Appendix 3, Table A3, for a comparison of NEMOMED8 outputs against
222 WOA13 observations, and a summary of the climatic anomalies used for predicting
223 species habitat suitabilities in 2020-2049 and in 2069-2098.

224

225 Environmental niche modelling and uncertainty due to species prevalences

226 To investigate the uncertainty due to the choice of the ENM, we used ten algorithms
227 that cover the complexity range of the commonly-used statistical methods (Merow et
228 al. 2014): three regression-based models: Generalized Linear Model (GLM),
229 Generalized Additive Model (GAM), Multivariate Adaptive Regression Splines
230 (MARS); one classification-based model: Flexible Discriminant Analysis (FDA); two
231 tree-based models: Random Forest (RF), Classification Tree Analysis (CTA); and
232 three machine learning models: Boosted Regression Trees (BRT), Artificial Neural
233 Networks (ANN), and Maximum entropy (MAXENT; Phillips et al. 2006). These nine
234 models require either presence/absence (P/A) data or presence-background (P/B)
235 data (for MAXENT, Yackulic et al. 2013; Guillera-Aroita et al. 2014). An additional
236 presence-only (P/O) ENM was also used: Surface Range Envelope (SRE, equivalent
237 to the Bioclim model; Busby 1991).

238 For the nine algorithms requiring P/A (or P/B) data, pseudo-absences (psA) were
239 randomly generated after defining both environmental and spatial weighting (Engler
240 et al. 2004; Hengl et al. 2009), to place them in regions of lowest environmental
241 suitability and far from the known presences (Hattab et al. 2014). The method
242 employed to generate pseudo-absences strongly impacts ENMs outputs, and should
243 be chosen in light of the species' ecological characteristics (Chefaoui and Lobo 2008;
244 VanDerWal et al. 2009; Barbet-Massin et al. 2012). Zooplankton is composed of
245 ectotherms whose population dynamics are tightly coupled to climate (Hays et al.
246 2005; Richardson 2008; Beaugrand et al. 2013), and whose individuals are passively
247 dispersed over very large spatial scales in relatively short time periods (Jönsson and
248 Watson 2016). Building on the results of Chefaoui and Lobo (2008), we chose to
249 employ the following method to randomly draw psA.

250 Firstly, the reverse environmental weighting was based on a P/O ecological niche
251 factor analysis (ENFA; Hirzel et al. 2002). This multivariate ordination technique
252 allocates a degree of similarity (ranging between 0 and 100) to each cell (at the
253 global scale for ENM calibration) by comparing the species environmental envelope
254 to the environmental conditions (using the three selected predictors). It therefore
255 provides an habitat suitability index (HSI) that was used together with the distance to
256 presences to produce the following probability distribution τ (Hengl et al. 2009):
257

$$258 \quad \tau_x = \left[\frac{d_x + (100 - HSI_x)}{2} \right]^2$$

259
260 with d_x being the distance to presences normalized by the maximum distance, and
261 pseudo-absences are increasingly drawn at the edge of low HSI values because of
262 the squared term. τ was used as a probability density function to randomly simulate
263 pseudo-absences in unsuitable habitats and further away from known presences. We
264 argue that this method allows to draw the psA in the environment that is theoretically
265 reachable for the studied species (as recommended by Barve et al. 2011) because at
266 decadal time scales, planktonic communities are well-connected anywhere in the
267 ocean, as recently demonstrated by Jönsson and Watson (2016).

268 The chosen number of psA also impacts ENMs projections (Barbet-Massin et al.
269 2012; Meynard et al. 2013). Considering that the regional occurrence data do not
270 allow to approximate each species' prevalences in the Mediterranean Sea (because
271 of the low surface coverage of scientific cruises), we chose to draw a varying number
272 of psA for each species. This allowed to investigate the relative amount of uncertainty
273 related to species prevalence. Different levels of species prevalences were
274 considered by increasing the ratio of drawn pseudo-absences over the number of
275 presences (which was kept constant at the number of observations): 1 (npsA = nP),
276 0.67 (npsA = 1.5*n), 0.5 (npsA = 2*nPres), 0.1 (npsA = 10*nP), and 0.02 (npsA =
277 50*nP). These 5 prevalence levels were finally used in the variance analysis (see
278 below) as an additional uncertainty factor, together with ENM choice, SRES, BF and
279 the ensuing interaction terms.

280 To account for the stochasticity in the psA generation process, 10 different psA
281 realisations were carried out for each species (so each species presents 50 P-psA
282 datasets). For every species and every ENMs algorithm, the 50 P/psA datasets were
283 split into a calibration set (80%) and a testing set (20%). Models were evaluated
284 according to the True Skill Statistic (TSS) criterion (Allouche et al. 2006) with a three-
285 fold cross-validation. See Supplementary material Appendix 4 and 5, Fig. A4-5, for
286 the species and the ENMs evaluation scores.

287
288 Mapping future shifts in species assemblages

289 P/A distribution maps were generated from the habitat suitabilities over the
290 Mediterranean Sea for each species (Fig. 1), and for each combination of ENM
291 (n=10), cross-validation runs (n=3), prevalence level (n=5), pseudo-absence
292 realisation (n=10) and hydrodynamical model's boundary forcings (n=6). This was
293 done for the two future time periods. Species assemblages (i.e. the sum of species
294 modelled as present or absent in each cell grid) were built by stacking all the species
295 P/A maps (according to the identity of the above-mentioned parameters). Species
296 assemblages for the baseline period were simulated in the same manner, but for a
297 single set of environmental conditions (WOA13 baseline climatologies).

298 By comparing the present to the future assemblages, indices of community shifts
299 related to α and β diversity were computed within each grid cell: difference in species
300 richness (Δ SR), and Jaccard's dissimilarity index (β_{jac}).

301 For each period, the sum of the species modelled as present was used to estimate
302 species richness. Δ SR was computed as the difference between future species
303 richness and the baseline species richness, and was used to assess whether climate
304 changes would promote or weaken copepod α diversity.

305 Pairwise Jaccard's dissimilarity index (ranging between 0 and 1) is given by:

306

$$307 \quad \beta_{jac} = \frac{b + c}{a + b + c}$$

308

309 where a is the number of species present at both time periods, b is the number of
310 species present in the baseline period only, and c is the number of species present in
311 the future time period only. It was used to assess the temporal changes in species
312 assemblages composition. In addition, by applying the framework of Baselga et al.
313 (2012), β_{jac} values were decomposed into its two additive components: nestedness
314 (β_{jne}) and turnover (β_{jtu}). The latter expresses species replacement without the
315 influence of Δ SR between time steps as follows:

316

$$317 \quad \beta_{jtu} = \frac{2\min(b, c)}{a + 2\min(b, c)}$$

318

319 The difference between β_{jac} and β_{jtu} expresses the nestedness component β_{jne}
320 that accounts for the amount of dissimilarity that is due to differences in richness
321 ($\beta_{jne} = \beta_{jac} - \beta_{jtu}$). It is formulated as follows:

322

$$323 \quad \beta_{jne} = \frac{\max(b, c) - \min(b, c)}{a + b + c} \times \frac{a}{a + 2\min(b, c)}$$

324

325 Moreover, the ratio between β_{jne} and β_{jtu} ($\beta_{ratio} = \beta_{jne} / \beta_{jac}$) was computed and
326 related to Δ SR in order to understand which component has the highest contribution
327 to future changes in the species assemblages (Dobrovolski et al. 2012; Albouy et al.
328 2012). For instance, a β_{ratio} value greater than 0.5 indicates that the observed
329 dissimilarity is driven by nestedness, which can occur under both increases or
330 decreases in richness. Alternatively, a value lower than 0.5 indicates the shift is
331 driven by species replacement. When Δ SR is positive and turnover drives the
332 dissimilarity in the assemblage, it means that climate change promotes diversity by
333 creating favourable conditions for species that were not present previously. When
334 Δ SR is positive and nestedness drives the dissimilarity, climate change promotes
335 richness while not changing the initial assemblage composition.

336

337 Processing novel climate conditions

338 To identify where niches are projected into novel combinations of environmental
339 predictors (Zurell et al. 2012; Mesgaran et al. 2014), cells where ENMs extrapolation
340 occurs were determined according to the species Multivariate Environmental
341 Similarity Surface (MESS; Elith et al. 2010). It enables to evaluate how dissimilar the
342 environment used for projecting the ENMs is from the species native range (i.e.
343 reference envelope used for ENMs calibration). The MESS maps present both

344 positive and negative values, the later indicating the cells where novel climate
345 conditions occur. Since the maps depend on the calibration dataset, MESS values
346 were computed for each species and for every combination of prevalence level and
347 future circulation model forcing conditions (i.e. SRES and BF, thus 30 maps per
348 species). The psA realisations or the ENMs' cross-evaluation runs do not significantly
349 affect the MESS, so they were not taken into account when identifying novel climate
350 conditions.

351 Within each cell, the species presenting negative MESS values were discarded from
352 the assemblage's species list, and changes in α and β diversity were computed
353 without them. The ratio of species being discarded was computed and mapped for
354 each prevalence and NEMOMED8 configuration (data not shown) in order to assess
355 where non analog climates have the strongest impact. In the cases where novel
356 conditions do not allow to predict changes in copepod diversity (because all species
357 had to be discarded from the assemblages), the corresponding cells were left blank
358 in the consensus projections and were ignored in the subsequent variance analysis
359 (see below). All analyses were also carried out while ignoring MESS outputs, but as it
360 did not alter the main results, only those obtained when accounting for non analog
361 climates are presented. Density distributions in future Mediterranean environmental
362 ranges were visually compared to the current ones to identify the combination of
363 predictors that may lead to the appearance of novel climate conditions.

364

365 Consensus projections and partitioning sources of uncertainties

366 To identify the dominant patterns in assemblages shifts, consensus maps were
367 drawn for each of the calculated indices by averaging their values within each cell
368 and across every model run. The associated standard deviation was used to assess
369 variability between runs as well as its spatial distribution over the basin.

370 Three-way ANOVA was used to assess the contributions of the different uncertainty
371 sources to the overall variability in Δ SR (Diniz-Filho et al. 2009; Garcia et al. 2012):
372 ENMs, emission scenario (SRES), circulation model boundary forcing (BF), species
373 prevalence, and the associated interaction terms. BF and SRES were treated
374 separately in the variance analyses because not all BF have been coupled with every
375 SRES. The relative amount of uncertainty attributable to the sources was estimated
376 as the proportion of sum of squares with respect to the total sum (Diniz-Filho et al.
377 2009; Garcia et al. 2012).

378 The three-way ANOVA was performed in a linear mixed-effect model framework that
379 allowed to account for the variation in effect size produced when iterating 3 cross-
380 validation runs within 10 psA realisations.

381 To further examine how projections differ under combinations of ENMs and ocean
382 model configurations, values of Δ SR were averaged to obtain consensus projections
383 for each combination of BF/SRES and ENMs (e.g. SRE-A2, MAXENT-B1ARF, GLM-
384 A2F etc.). Similarity between these projections were assessed by analysing their
385 loadings on the first principal component of an unscaled Principal Component
386 Analysis (PCA; Legendre and Legendre 2012).

387 All statistical analyses were conducted under the R environment (R Core Team
388 2014) using the biomod2 package (Thuiller et al. 2013) for ENMs and the betapart
389 package (Baselga and Orme 2012) for biodiversity indices' estimates.

390

391 **Results**

392 Consensus patterns of α and β diversity show that species nestedness with
393 decreases in richness is the main pattern driving the dissimilarity between present

394 and future copepod assemblages ($\Delta SR < 0$ and $\beta ratio < 0.5$; Fig. 2). Indeed, 91.63%
395 and 95.85% of the cells exhibit a decline in species richness by 2020-2049 and 2069-
396 2098 respectively. Mean ΔSR is -2.13 for the mid-century and -5.13 for the end-of-
397 century period (mean SR for the baseline period being 75.83). The projected patterns
398 are spatially structured. The largest decreases in richness are observed in the
399 eastern Mediterranean (Fig. 2c-d). The few cells that show positive ΔSR (8.37% by
400 2020-2049; 4.15% by 2069-2098) are located in the northwestern area (Gulf of Lions,
401 Ligurian Sea), the Alboran Sea, and the northernmost parts of the Adriatic and the
402 Aegean Seas (Fig. 2c-d), which are characterised by milder temperature and lower
403 salinity waters, both now and in the future. Gains and losses in richness are mainly
404 associated with nestedness. Most of Mediterranean cells show mean $\beta ratio$ values
405 higher than 0.5 for 2020-2049 (total mean $\beta ratio = 0.63$). By 2069-2098, 98,31% of
406 the cells exhibit a higher contribution of nestedness than turnover in assemblages'
407 dissimilarity (total mean $\beta ratio = 0.77$). Gains in species richness associated with
408 turnover only appear in the Alboran and Marmara Seas by 2069-2098 (Fig. 2d).
409 As shown on Fig. 2c,d, non analog conditions occur in the central Aegean Sea and
410 the easternmost part of the Levantine basin by 2069-2098, due to non analog SSS
411 values (future SST and σSST were always within the range of the calibration data).
412 The entire Levantine basin is actually affected by novel salinity conditions, as nearly
413 50% of the species had to be discarded from the assemblages, depending on the
414 considered model forcings and prevalences (data not shown).

415
416 Standard deviations of ΔSR were computed within each cell to assess its variability
417 across runs (Fig. 3). The amplitude of the predicted losses in species richness scales
418 with its variability ($R^2 = 0.54$, $P\text{-value} < 2.2 \times 10^{-16}$), which is also true for the cells that
419 exhibit positive ΔSR value ($R^2 = 0.59$, $P\text{-value} < 2.2 \times 10^{-16}$). The strongest differences
420 in richness and assemblage dissimilarity rates occur in the eastern part of the
421 Mediterranean basin. Uncertainties across model runs are therefore larger for these
422 regions.

423
424 Three-way ANOVA based on linear mixed-effects models helped disentangling the
425 relative contribution of different sources of uncertainty. For both future time periods,
426 the choice of the ENMs explains most of the variability in projections of ΔSR (Fig.
427 4a,b). The same result was obtained for the dissimilarity indices, and are therefore
428 not presented. On average, the relative contribution of ENMs to the total sum of
429 squares increases from 72.68% in 2020-2049 to 74.14% in 2069-2098, when
430 accounting for the choice of BF. When accounting for SRES rather than BF, ENMs'
431 average contribution decreases from 82.25% in 2020-2049 to 68.66% in 2069-2098.
432 The second most important contributing factors are the interaction terms, indicating
433 divergent ENMs responses according to different BF and SRES configurations
434 (23.16% in 2020-2049 and 17.96% in 2069-2098 when accounting for BF; 14.44% in
435 2020-2049 and 19.81% in 2069-2098 with SRES). The choice of the BF, of the
436 SRES, or of the prevalence level, always show mean relative contributions lower
437 than 6%.

438
439 Predicted shifts in species assemblages are mainly driven by the ENMs and their
440 interactions with either the BF or the SRES. Therefore similarities across the ENMs'
441 average ΔSR projections were examined through a PCA. The first two Principal
442 Components (PC1 and PC2) explain 87.73% of total variance. However the SRE
443 predictions' relative contribution to PC1 and PC2 reaches 48.85% (Fig. 5a). Since all

444 PCs are orthogonal to one another and the P/A ENMs are contributing to non-
445 significant components, SRE projections should not be averaged together with the
446 other methods in an ensemble forecasting framework. When averaging SRE
447 projections, higher consensus values of negative Δ SR and nestedness are obtained
448 (Fig. 5b). Mean Δ SR in the Mediterranean Sea for 2069-2098 decreases to -11.21
449 while the mean β ratio increases up to 0.95. The proportion of cells exhibiting strictly
450 positive Δ SR slightly increases from 4.15% to 7.85%.

451 A second PCA was performed with the P/psA models' projections only. Again, the
452 loading coordinates are used to explore their degree of similarity in their Δ SR
453 forecasts (Fig. 6). Examining the maps of mean Δ SR for each P/psA ENM revealed
454 that the loadings along PC1 (64.00% of total variance) are to be interpreted as an
455 increasing gradient in the predicted species loss. All nine p/psA ENMs present the
456 same spatial pattern in species richness increases, while the range of their predicted
457 decreases vary. ENMs with higher loadings on PC1 are those that predict greater
458 declines in richness (Fig. 6). MARS projections are the most pessimistic regarding
459 Δ SR values, with all its configurations having higher loadings than the other ENMs.
460 The more pessimistic models include MARS, CTA and ANN (in order of pessimism).
461 The least pessimistic forecasts are produced by the remaining models: MAXENT,
462 RF, FDA, GAM, GBM and GLM.

463 The ENMs predicting the most negative values of Δ SR are the ones with the most
464 variability in loadings along PC1 (MARS followed by CTA and ANN). A significant
465 correlation was found between the ENMs average loadings and the range of loadings
466 (the distance between the least conservative configuration (A2ARF) and the most
467 conservative one (B1ARF) ($R^2 = 0.82$, P-value < 0.001). This indicates the most
468 pessimistic ENMs are also the most sensitive to the choice of the BF and SRES.

469

470 **Discussion**

471 In the present study, we explored the uncertainties in future composition changes in
472 Mediterranean copepod assemblages. Different combinations of species
473 prevalences, ENMs, circulation model boundary forcings, and emission scenarios
474 were used to forecast shifts in species assemblages for the 21st century. Our results
475 have implications for studies aiming to forecast changes in habitat suitability for
476 planktonic species with ENMs, from both technical and theoretical perspectives.

477

478 **Main sources of uncertainties**

479 Our results are in agreement with previous studies (Diniz-Filho et al. 2009; Buisson
480 et al. 2010; Garcia et al. 2012) that documented the variability in forecasts related to
481 the differences between ENMs outputs (Fig. 4). The main divergence occurs
482 between the SRE model, the sole P/O ENM considered here, and the other ENMs
483 that were all based on P/psA (or P/B for MAXENT) data (Fig. 5).

484 Dissimilarity between present and future assemblages was much greater when
485 predicted by the SRE than with the other ENMs, but nestedness in species losses
486 remained the dominant pattern driving the dissimilarity. Previous studies comparing
487 P/O to P/A (or P/psA and P/B) methodologies consistently found SRE models to
488 underestimate species ranges, which translated into more pessimistic forecasts of
489 changes in richness (Pearson et al. 2006; Hijmans and Graham 2006). The SRE
490 uses percentile distribution to draw a rectangular "box" (a range envelope) around
491 the presence data in environmental space (Busby 1991). SRE projections depend on
492 the overlap between the defined envelope and the future conditions, whereas P/A
493 models (e.g. GLM-derived response curves) allow to recognise favourable areas

494 even beyond the range of the observed presences. The large discrepancies between
495 the SRE and the P/psA models are also due to the methodology chosen to generate
496 psA. Environmental and spatial weightings were applied such that psA were
497 assigned in unsuitable areas as far as possible from known presences (Hengl et al.
498 2009). Therefore the environmental range captured by the SRE is much narrower
499 than the one captured by the other models.

500 The similarity between correlative ENMs along the first component of a PCA can be
501 related to the similarity between the models' algorithms (Fig. 6). Regression-based
502 methods forecasts are quite similar to one another (GLM, GAM, FDA). The same is
503 evidenced for complex classification-trees (GBM, RF). GBM predictions are similar to
504 regression models because the algorithm used here is equivalent to boosted
505 regression trees (Ridgeway 1999; Friedman 2001). MAXENT projections are similar
506 to both GBM's and regression-based models', as its core algorithm contains a
507 machine-learning piece (Elith et al. 2011), and it may be close to GLMs depending on
508 the tuning of its parameters (Guillera-Arroita et al. 2014; Halvorsen et al. 2015).
509 MARS-based projections forecasted the greatest rates of species loss among P/psA
510 models. It may seem surprising that MARS projections were not closer to regression-
511 based models since they rely on a non-parametric regression procedure that is often
512 seen as an extension of GLMs and GAMs (Friedman 1991; Franklin 2009). The
513 greater species losses predicted by MARS models could be due to the first-order
514 interactions that were enabled between the predictive variables (they were disabled
515 for the other models).

516 The interaction terms between ENMs and BF, and/or the choice of the SRES, were
517 identified as the second uncertainty-generating factor (Fig. 4). The BF can have an
518 important but very local impact, meaning it is restricted to the few cells located near
519 the forcing fluxes (e.g. the Alboran Sea for the Atlantic hydrography, and the
520 Northern Aegean sea for the river runoff, since the Black Sea is treated as a river in
521 this circulation model). The sensitivity to the choice of the SRES slightly increases
522 between the two future periods (Fig. 4b) consistently with the response of the
523 physical variables in climate scenarios. Due to the long lifetime of anthropogenic CO₂
524 in the atmosphere, the magnitude of oceanic response is smaller in the first half of
525 the 21st century.

526 Our results have important implications for interpreting previous studies that have
527 predicted shifts in habitat suitability for fishes over the Mediterranean continental
528 shelf (Ben Rais Lasram et al. 2010; Albouy et al. 2012). Their results were all based
529 on species habitat suitabilities that were estimated through a weighted average
530 consensus across seven ENMs, including the SRE. Combining the SRE in ensemble
531 predictions will lead to less conservative changes (i.e. higher predicted rates of
532 species loss) than excluding it based on the evaluation criterion score (which is the
533 most common criterion for weight attribution). From the present results, we argue that
534 P/O and P/psA (or P/B) models outputs should be compared (e.g. with a PCA) before
535 being mixed together as they rely on different data and assumptions, and are likely to
536 model different components of the species niche (Brotons et al. 2004; Sillero 2011).
537 Indeed, the PCA identified these two types of methods as two different "visions" of
538 the species niches, both leading to two different scenarios of biodiversity change.

539
540 Guidelines for modelling zooplankton with ENMs

541 Modelling habitat suitabilities through P/O or P/A methods holds different implications
542 depending on the ecological properties of the species (Hernandez et al. 2006; Tsoar
543 et al. 2007; Jimenez-Valverde et al. 2008). One group of methods might be better

544 suited than another according to the taxa of interest. Brotons et al. (2004) suggested
545 that P/O models may be more accurate for species that are far from equilibrium with
546 their environment. For several reasons, we argue that correlative models, based on
547 environmentally-weighted psA, are appropriate for modelling zooplanktonic taxa.
548 First, they are short-lived ectotherms whose physiology and population dynamics are
549 tightly coupled with climate variability (Hays et al. 2005; Richardson 2008). Sunday et
550 al. (2011; 2012) showed that the spatial ranges of marine ectotherms closely match
551 their thermal tolerance limits. Most of the zooplankton are not commercially exploited,
552 so in absence of direct human harvesting they are likely to be near equilibrium with
553 the environment, and their geographical distribution is a good indicator of their abiotic
554 preferences.

555 Copepods exhibit very broad latitudinal ranges (Razouls et al. 2005-2016) which
556 result from both wide environmental preferences and huge dispersal potential due to
557 turbulent oceanic circulation (Jönsson and Watson 2016). However, the potentially
558 worldwide distributions of these organisms (Finlay 2002; Cermeño and Falkowski
559 2009; de Vargas et al. 2015), combined with spatially (and temporally) biased data
560 sets, limit the ENMs' capacity to link species occurrences to environmental predictors
561 properly. In consideration of the datasets attributes (large spatial autocorrelation due
562 to sampling biases coarse resolution etc.), future niche modelling studies should not
563 focus on using complex ENM algorithms. Since they are likely to fit spurious
564 relationships, or natural stochasticity (visible through noisy response curves), and
565 thus to be less transferable in time and space (Jimenez-Valverde et al. 2008;
566 Heinanen et al. 2012; Merow et al. 2014).

567 We advocate that P/psA methods applied to zooplankton should be coupled with
568 environmentally-weighted simulations of pseudo-absences because (i) absence data
569 are impossible to ascertain in the plankton realm, and (ii) marine ectotherms are at
570 equilibrium with their environments. Multiple methods of model evaluation and
571 comparison should be considered (Brun et al. 2016), such as niche transferability
572 tests in space and time (niche hindcasting), or comparison with mechanistic models
573 outputs and/or response curves from laboratory experiments. Habitat suitability
574 estimates along environmental gradients will be of great use for marine ecologists as
575 they can easily be coupled with functional traits data (Benedetti et al. 2016) to better
576 explore trait biogeography, and their link with ecosystem functioning (Albouy et al.
577 2015).

578

579 Future shifts in zooplankton surface assemblages

580 Previous studies modelling climate change impacts on zooplankton have generally
581 focused on changes of habitat suitability or species richness (Reygondeau and
582 Beaugrand 2011; Beaugrand et al. 2015). Here, we extended the use of planktonic
583 niche models for measuring β diversity. We predicted that climate change might lead
584 to a loss of copepod diversity throughout most of the surface of the Mediterranean
585 Sea (although some northern regions exhibit increases in species richness), with
586 nestedness as the main pattern driving the dissimilarity between present and future
587 assemblages (Fig. 2). Our results imply that future copepod assemblages in most of
588 the surface Mediterranean Sea will be composed of less species, all remnants being
589 present in the initial assemblages. Areas of potential future increases in copepod
590 diversity are restricted to the coldest regions: the Gulf of Lions, the Alboran Sea and
591 the northern Adriatic and Aegean Seas. Again, our predictions imply that climate
592 change might make these areas suitable for new species, without removing the ones
593 present in the initial assemblages.

594 This pattern may be explained by the northward shifts of temperature and salinity
595 sensitive species towards the Gulf of Lions, and the northern Adriatic and Aegean
596 Seas. These results are in agreement with the rate of climate change estimated by
597 Burrows et al. (2014), who tracked SST isotherms modelled by a global ocean model
598 that was forced by the RCP 8.5 emission scenario.

599 Nestedness was also the dominant pattern in forecasted changes in Mediterranean
600 coastal fish assemblages (Albouy et al. 2012). However, the rates of changes in
601 species richness we found for copepods are arguably much lower. In addition,
602 Albouy et al. (2012) predicted higher proportions of cells displaying increases in
603 species richness, and in more diverse locations throughout the basin. They predicted
604 increases in fish diversity in the central Adriatic, the central and northern Aegean,
605 and the coastal Levantine. Meanwhile, we predict higher diversity losses in these
606 regions, that will experience the strongest rates of warming and saltening (Adloff et
607 al. 2015).

608 The fact that planktonic copepods present broader environmental niches, compared
609 to coastal fishes, may explain this discrepancy. The considered fishes include
610 endemic species with much narrower thermal amplitudes (Ben Rais Lasram et al.
611 2010) than planktonic species characterized by global scale distributions. This is in
612 line with the results from Mediterranean coastal time series that demonstrated the
613 strong resilience of copepod communities to highly variable conditions, over pluri-
614 decadal scales (Siokou-Frangou et al. 2010; Mazzocchi et al. 2011).

615 The comparison between our results and previous studies conducted on other
616 components of Mediterranean marine ecosystems implies that different components
617 of the pelagic food web may not respond to climate changes in unique ways.
618 Consequently, predicting climate-induced shifts in ecosystems requires to account for
619 multiple trophic levels.

620

621 Limitations

622 A notable limitation of our study is that we were unable to test the relative
623 contribution of the choice of the regional circulation model because of data
624 availability. Previous studies have shown this factor to be the second-most important
625 in explaining variability across predictions, persistently ranking in front of interaction
626 terms (Diniz-Filho et al. 2009; Buisson et al. 2010; Garcia et al. 2012). Consequently,
627 it is reasonable to believe that it could represent a second-order uncertainty factor in
628 our case as well. But it is not likely to overstep ENMs as the major source of
629 uncertainty (Garcia et al. 2012). It is noteworthy that different regional ocean
630 circulation models generally agree on the future impacts of climate change on the
631 overall Mediterranean circulation and physical conditions (Dubois et al. 2012; Gualdi
632 et al. 2013). So we are confident our consensus patterns of shifts might not
633 drastically change when switching to another regional circulation model.

634 Additionally, zooplankton is known to perform diel vertical migrations that can span
635 several hundreds of meters depending on the species (Roe 1974; Ohman 1990). So
636 it is crucial to note that our habitat suitability predictions are only valid for the surface
637 waters of the Mediterranean Sea. Changes in the species surface habitat suitability
638 could lead to horizontal spatial range shifts as the species track optimal growth
639 conditions (Sunday et al. 2012; Poloczanska et al. 2013), but it could also trigger a
640 deepening of their distribution (Dulvy et al. 2008). The exact depth of the species
641 occurrences is difficult to establish for each observation which limits the development
642 of three-dimensional niche models (Bentlage et al. 2013). Still, we point out that the
643 majority of the occurrence data used here comes from surface layers (0-200m

644 depth), and that only a few of the studied copepod species do perform large vertical
645 migrations in the Mediterranean basin (Scotto di Carlo et al. 1984; Benedetti et al.
646 2016).

647

648 **Acknowledgments**

649 *Financial support was provided by the EC FP7 PERSEUS Project (Grant. Agr.*
650 *287600), the MerMex (Marine Ecosystems Response in the Mediterranean*
651 *Experiment)/MISTRALS French National Program, through the PlankMed action, and*
652 *by the Climate-KIC initiative of the European Institute of Innovation & Technology*
653 *(EIT) through a PhD grant given to F.B. This work is part of the Med-CORDEX*
654 *initiative (www.medcordex.eu) supported by the HyMeX programme*
655 *(www.hymex.org). The authors are grateful to Jean-Olivier Irisson and Guilhem*
656 *Marre for their numerical inputs all along the study. We are most grateful to Tarek*
657 *Hattab for his help regarding the pseudo-absence generation algorithm. We also*
658 *thank Samuel Somot. Special thanks are given to Traci Erin Cox for her corrections*
659 *on the text. We are also grateful to Christine Meynard and anonymous reviewers for*
660 *their comments on the manuscript.*

661 **References**

- 662 Adloff, F. et al. 2015. Mediterranean Sea response to climate change in an ensemble of twenty first century
663 scenarios. — *Climate Dynamics* 1-28.
- 664 Albouy, C. et al. 2012. Combining projected changes in species richness and composition reveals climate change
665 impacts on coastal Mediterranean fish assemblages. — *Global Change Biology* 18: 2995-3003.
- 666 Albouy, C. et al. 2014. From projected species distribution to food- web structure under climate change. — *Global
667 change biology* 20: 730-741.
- 668 Albouy, C. et al. 2015. Projected impacts of climate warming on the functional and phylogenetic components of
669 coastal Mediterranean fish biodiversity. — *Ecography* 38: 681-689.
- 670 Allouche, O. et al. 2006. Assessing the accuracy of species distribution models: prevalence, kappa and the true
671 skill statistic (TSS). — *Journal of Applied Ecology* 43: 1223-1232.
- 672 Anderson, M. J. et al. 2011. Navigating the multiple meanings of β diversity: a roadmap for the practicing
673 ecologist. — *Ecology letters* 14: 19-28.
- 674 Araújo, M. B. et al. 2005. Validation of species-climate impact models under climate change. — *Global Change
675 Biology* 11: 1504-1513.
- 676 Araújo, M. B. and Luoto, M. 2007. The importance of biotic interactions for modelling species distributions under
677 climate change. — *Global Ecology and Biogeography* 16: 743-753.
- 678 Araújo, M. B. and New, M. 2007. Ensemble forecasting of species distributions. — *Trends in ecology & evolution*
679 22: 42-47.
- 680 Araújo, M. B. and Peterson, A. T. 2012. Uses and misuses of bioclimatic envelope modeling. — *Ecology* 93:
681 1527-1539.
- 682 Barbet-Massin, M. et al. 2012. Selecting pseudo-absences for species distribution models: how, where and how
683 many? — *Methods in Ecology and Evolution* 3: 327-338.
- 684 Barton, A. D. et al. 2016. Anthropogenic climate change drives shift and shuffle in North Atlantic phytoplankton
685 communities. — *Proceedings of the National Academy of Sciences* 113: 2964-2969.
- 686 Barve, N. et al. 2011. The crucial role of the accessible area in ecological niche modeling and species distribution
687 modeling. — *Ecological Modelling* 222: 1810-1819.
- 688 Baselga, A. 2010. Partitioning the turnover and nestedness components of beta diversity. — *Global Ecology and
689 Biogeography* 19: 134-143.
- 690 Baselga, A. and Orme, C. D. L. 2012. betapart: an R package for the study of beta diversity. — *Methods in
691 Ecology and Evolution* 3: 808-812.
- 692 Bateman, B. L. et al. 2012. Biotic interactions influence the projected distribution of a specialist mammal under
693 climate change. — *Diversity and Distributions* 18: 861-872.
- 694 Beaugrand, G. et al. 2002. Diversity of calanoid copepods in the North Atlantic and adjacent seas: species
695 associations and biogeography. — *Marine Ecology Progress Series* 232:
- 696 Beaugrand, G. et al. 2010. Marine biodiversity, ecosystem functioning, and carbon cycles. — *Proceedings of the
697 National Academy of Sciences* 107: 10120-10124.
- 698 Beaugrand, G. et al. 2011. A new model to assess the probability of occurrence of a species based on presence-
699 only data. — *Marine Ecology Progress Series* 424: 175-190.
- 700 Beaugrand, G. et al. 2013. Applying the concept of the ecological niche and a macroecological approach to
701 understand how climate influences zooplankton: advantages, assumptions, limitations and requirements. —
702 *Progress in Oceanography* 111: 75-90.
- 703 Beaugrand, G. et al. 2015. Future vulnerability of marine biodiversity compared with contemporary and past
704 changes. — *Nature Climate Change* 5: 695-701.
- 705 Beaugrand, G. and Kirby, R. R. 2010. Climate, plankton and cod. — *Global Change Biology* 16: 1268-1280.
- 706 Beaumont, L. J. et al. 2008. Why is the choice of future climate scenarios for species distribution modelling
707 important? — *Ecology Letters* 11: 1135-1146.
- 708 Bellard, C. et al. 2012. Impacts of climate change on the future of biodiversity. — *Ecology Letters* 15: 365-377.
- 709 Ben Rais Lasram, F. et al. 2010. The Mediterranean Sea as a "cul de sac" for endemic fishes facing climate
710 change. — *Global Change Biology* 16: 3233-3245.
- 711 Benedetti, F. et al. 2016. Identifying copepod functional groups from species functional traits. — *Journal of
712 Plankton Research* 38: 159-166.
- 713 Bentlage, B. et al. 2013. Plumbing the depths: extending ecological niche modelling and species distribution
714 modelling in three dimensions. — *Global Ecology and Biogeography* 22: 952-961.
- 715 Beuvier, J. et al. 2010. Modeling the Mediterranean Sea interannual variability during 1961-2000: focus on the
716 Eastern Mediterranean transient. — *Journal of Geophysical Research: Oceans* (1978-2012) 115:C8
- 717 Bianchi, C. N. and Morri, C. 2000. Marine Biodiversity of the Mediterranean Sea: Situation, Problems and
718 Prospects for Future Research. — *Marine Pollution Bulletin* 40: 367-376.
- 719 Blanco-Bercial, L. et al. 2011. Comparative phylogeography and connectivity of sibling species of the marine
720 copepod *Clausocalanus* (Calanoida). — *Journal of Experimental Marine Biology and Ecology* 404: 108-115.
- 721 Brotons, L. et al. 2004. Presence-absence versus presence-only modelling methods for predicting bird habitat
722 suitability. — *Ecography* 27: 437-448.
- 723 Brotons, L. 2014. Species Distribution Models and Impact Factor Growth in Environmental Journals:
724 Methodological Fashion or the Attraction of Global Change Science. — *PLoS ONE* 9:
- 725 Brun, P. et al. 2015. Ecological niches of open ocean phytoplankton taxa. — *Limnology and Oceanography* 60:
726 1020-1038.

727 Brun, P. et al. 2016. The predictive skill of species distribution models for plankton in a changing climate. —
728 Global Change Biology n/a-n/a.

729 Buisson, L. et al. 2010. Uncertainty in ensemble forecasting of species distribution. — Global Change Biology 16:
730 1145-1157.

731 Burrows, M. T. et al. 2014. Geographical limits to species-range shifts are suggested by climate velocity. —
732 Nature 507: 492-495.

733 Busby, J. R. 1991. BIOCLIM-a bioclimate analysis and prediction system. — Plant Protection Quarterly (Australia)

734 Cermeño, P. and Falkowski, P. G. 2009. Controls on diatom biogeography in the ocean. — Science 325: 1539-
735 1541.

736 Chefaoui, R. M. and Lobo, J. M. 2008. Assessing the effects of pseudo-absences on predictive distribution model
737 performance. — Ecological Modelling 210: 478-486.

738 Cheung, W. W. et al. 2010. Large- scale redistribution of maximum fisheries catch potential in the global ocean
739 under climate change. — Global Change Biology 16: 24-35.

740 Chust, G. et al. 2013. Are Calanus spp. shifting poleward in the North Atlantic? A habitat modelling approach. —
741 ICES Journal of Marine Science: Journal du Conseil 147.

742 Coll, M. et al. 2012. The Mediterranean Sea under siege: spatial overlap between marine biodiversity, cumulative
743 threats and marine reserves. — Global Ecology and Biogeography 21: 465-480.

744 Coma, R. et al. 2009. Global warming-enhanced stratification and mass mortality events in the Mediterranean. —
745 Proceedings of the National Academy of Sciences 106: 6176-6181.

746 Costalago, D. et al. 2014. Seasonal comparison of the diets of juvenile European anchovy *Engraulis encrasicolus*
747 and sardine *Sardina pilchardus* in the Gulf of Lions. — Journal of Sea Research 89: 64-72.

748 Dam, H. G. 2013. Evolutionary Adaptation of Marine Zooplankton to Global Change. — Annual Review of Marine
749 Science 5: 349-370.

750 Danovaro, R. et al. 2004. Biodiversity response to climate change in a warm deep sea. — Ecology Letters 7: 821-
751 828.

752 de Vargas, C. et al. 2015. Eukaryotic plankton diversity in the sunlit ocean. — Science 348: 1261605, 1-11.

753 Diniz-Filho, J. A. F. et al. 2009. Partitioning and mapping uncertainties in ensembles of forecasts of species
754 turnover under climate change. — Ecography 32: 897-906.

755 Dobrovolski, R. et al. 2012. Climatic history and dispersal ability explain the relative importance of turnover and
756 nestedness components of beta diversity. — Global Ecology and Biogeography 21: 191-197.

757 Dubois, C. et al. 2012. Future projections of the surface heat and water budgets of the Mediterranean Sea in an
758 ensemble of coupled atmosphere-ocean regional climate models. — Climate Dynamics 39: 1859-1884.

759 Dulvy, N. K. et al. 2008. Climate change and deepening of the North Sea fish assemblage: a biotic indicator of
760 warming seas. — Journal of Applied Ecology 45: 1029-1039.

761 Elith, J. et al. 2006. Novel methods improve prediction of species' distributions from occurrence data. —
762 Ecography 29: 129-151.

763 Elith, J. and Graham, C. H. 2009. Do they? How do they? WHY do they differ? On finding reasons for differing
764 performances of species distribution models. — Ecography 32: 66-77.

765 Elith, J. and Leathwick, J. R. 2009. Species distribution models: ecological explanation and prediction across
766 space and time. — Annual Review of Ecology, Evolution, and Systematics 40: 677.

767 Elith, J. et al. 2010. The art of modelling range- shifting species. — Methods in Ecology and Evolution 1: 330-342.

768 Elith, J. et al. 2011. A statistical explanation of MaxEnt for ecologists. — Diversity and Distributions 17: 43-57.

769 Engler, R. et al. 2004. An improved approach for predicting the distribution of rare and endangered species from
770 occurrence and pseudo- absence data. — Journal of Applied Ecology 41: 263-274.

771 Finlay, B. J. 2002. Global dispersal of free-living microbial eukaryote species. — Science 296: 1061-1063.

772 Franklin, J. 2009. Mapping species distributions: spatial inference and prediction. — Cambridge University Press.

773 Friedman, J. H. 1991. Multivariate Adaptive Regression Splines. — The Annals of Statistics 19: 1-67.

774 Friedman, J. H. 2001. Greedy function approximation: a gradient boosting machine. — Annals of statistics 1189-
775 1232.

776 Garcia, R. A. et al. 2012. Exploring consensus in 21st century projections of climatically suitable areas for African
777 vertebrates. — Global Change Biology 18: 1253-1269.

778 Garrabou, J. et al. 2009. Mass mortality in Northwestern Mediterranean rocky benthic communities: effects of the
779 2003 heat wave. — Global Change Biology 15: 1090-1103.

780 Gattuso, J.-P. et al. 2015. Contrasting futures for ocean and society from different anthropogenic CO2 emissions
781 scenarios. — Science 349: aac4722.

782 Giorgi, F. 2006. Climate change hot-spots. — Geophysical Research Letters 33: L08707.

783 Goberville, E. et al. 2015. Uncertainties in the projection of species distributions related to general circulation
784 models. — Ecology and evolution 5: 1100-1116.

785 Gualdi, S. et al. 2013. The CIRCE simulations: regional climate change projections with realistic representation of
786 the Mediterranean Sea. — Bulletin of the American Meteorological Society 94: 65-81.

787 Guillera-Arroita, G. et al. 2014. Maxent is not a presence-absence method: a comment on Thibaud et al. —
788 Methods in Ecology and Evolution 5: 1192-1197.

789 Guisan, A. and Zimmermann, N. E. 2000. Predictive habitat distribution models in ecology. — Ecological
790 modelling 135: 147-186.

791 Guisan, A. and Thuiller, W. 2005. Predicting species distribution: offering more than simple habitat models. —
792 Ecology Letters 8: 993-1009.

793 Halvorsen, R. et al. 2015. Opportunities for improved distribution modelling practice via a strict maximum
794 likelihood interpretation of MaxEnt. — *Ecography* 38: 172-183.
795 Harris, R. M. B. et al. 2014. Climate projections for ecologists. — *Wiley Interdisciplinary Reviews: Climate Change*
796 5: 621-637.
797 Hattab, T. et al. 2014. Towards a better understanding of potential impacts of climate change on marine species
798 distribution: a multiscale modelling approach. — *Global Ecology and Biogeography* 23: 1417-1429.
799 Hays, G. C. et al. 2005. Climate change and marine plankton. — *Trends in Ecology & Evolution* 20: 337-344.
800 Heinänen, S. et al. 2012. High resolution species distribution models of two nesting water bird species: a study of
801 transferability and predictive performance. — *Landscape ecology* 27: 545-555.
802 Hengl, T. et al. 2009. Spatial prediction of species' distributions from occurrence-only records: combining point
803 pattern analysis, ENFA and regression-kriging. — *Ecological Modelling* 220: 3499-3511.
804 Hernandez, P. A. et al. 2006. The effect of sample size and species characteristics on performance of different
805 species distribution modeling methods. — *Ecography* 29: 773-785.
806 Hijmans, R. J. and Graham, C. H. 2006. The ability of climate envelope models to predict the effect of climate
807 change on species distributions. — *Global Change Biology* 12: 2272-2281.
808 Hinder, S. L. et al. 2014. Multi- decadal range changes vs. thermal adaptation for north east Atlantic oceanic
809 copepods in the face of climate change. — *Global change biology* 20: 140-146.
810 Hirzel, A. et al. 2002. Ecological-niche factor analysis: how to compute habitat-suitability maps without absence
811 data? — *Ecology* 83: 2027-2036.
812 Hoegh-Guldberg, O. and Bruno, J. F. 2010. The impact of climate change on the world's marine ecosystems. —
813 *Science* 328: 1523-1528.
814 Hutchinson, G. E. 1957. Concluding remarks. *Cold Spring Harbor Symposia on Quantitative Biology*. Cold Spring
815 Harbor Laboratory Press, pp. 415-427.
816 IPCC 2007. *Climate change 2007: the physical science basis. Contribution of working group I to the fourth*
817 *assessment report of the intergovernmental panel on climate change*. Cambridge University Press, Cambridge.
818 IPCC 2013. *Climate change 2013: the physical science basis. Working group I contribution to the fifth assessment*
819 *report of the intergovernmental panel on climate change*. Cambridge University Press, Cambridge.
820 Irwin, A. J. et al. 2012. Phytoplankton niches estimated from field data. — *Limnology and Oceanography* 57: 787.
821 Jiménez-Valverde, A. et al. 2008. Not as good as they seem: the importance of concepts in species distribution
822 modelling. — *Diversity and distributions* 14: 885-890.
823 Jönsson, B.F. and Watson, J.R. 2016. The timescales of global-surface ocean connectivity. — *Nature*
824 *Communications* 7:11239, DOI: 10.1038/ncomms11239
825 Legendre, P. and Legendre, L. 2012. *Numerical ecology*. — Elsevier.
826 Levitus, S. et al. 2013. The World Ocean Database. — *Data Science Journal* 12: WDS229-WDS234.
827 Mackas, D. et al. 2012. Changing zooplankton seasonality in a changing ocean: Comparing time series of
828 zooplankton phenology. — *Progress in Oceanography* 97: 31-62.
829 Mauchline, J. 1998. *The biology of calanoid copepods*. — *Advances in Marine Biology* 33
830 Mazzocchi, M. G. et al. 2011. Zooplankton associations in a Mediterranean long-term time-series. — *Journal of*
831 *Plankton Research* 33: 1163-1181.
832 Mazzocchi, M. et al. 2014. Regional and seasonal characteristics of epipelagic mesozooplankton in the
833 Mediterranean Sea based on an artificial neural network analysis. — *Journal of Marine Systems* 135: 64-80.
834 Merow, C. et al. 2014. What do we gain from simplicity versus complexity in species distribution models? —
835 *Ecography* 37: 1267-1281.
836 Mesgaran, M. B. et al. 2014. Here be dragons: a tool for quantifying novelty due to covariate range and
837 correlation change when projecting species distribution models. — *Diversity and Distributions* 20: 1147-1159.
838 Meynard, C. N. and Kaplan, D. M. 2013. Using virtual species to study species distributions and model
839 performance. — *Journal of Biogeography* 40: 1-8.
840 Myers, N. et al. 2000. Biodiversity hotspots for conservation priorities. — *Nature* 403: 853-858.
841 Ohman, M. D. 1990. The demographic benefits of diel vertical migration by zooplankton. — *Ecological*
842 *Monographs* 257-281.
843 Nowaczyk, A. et al. 2011. Distribution of epipelagic metazooplankton across the Mediterranean Sea during the
844 summer BOUM cruise. — *Biogeosciences* 8: 2159-2177.
845 Owens, H. L. et al. 2012. Predicting suitable environments and potential occurrences for coelacanths (*Latimeria*
846 *spp.*). — *Biodiversity and Conservation* 21: 577-587.
847 Pearson, R. G. and Dawson, T. P. 2003. Predicting the impacts of climate change on the distribution of species:
848 are bioclimate envelope models useful? — *Global Ecology and Biogeography* 12: 361-371.
849 Pearson, R. G. et al. 2006. Model-based uncertainty in species range prediction. — *Journal of Biogeography* 33:
850 1704-1711.
851 Perry, A. L. et al. 2005. Climate change and distribution shifts in marine fishes. — *Science* 308: 1912-1915.
852 Phillips, S. J. et al. 2006. Maximum entropy modeling of species geographic distributions. — *Ecological modelling*
853 190: 231-259.
854 Pinkernell, S. and Beszteri, B. 2014. Potential effects of climate change on the distribution range of the main
855 silicate sinker of the Southern Ocean. — *Ecology and evolution* 4: 3147-3161.
856 Pinsky, M. L. et al. 2013. Marine taxa track local climate velocities. — *Science* 341: 1239-1242.
857 Poloczanska, E. S. et al. 2013. Global imprint of climate change on marine life. — *Nature Climate Change* 3: 919-
858 925.

859 R Core Team (2014). R: A language and environment for statistical computing. R Foundation for Statistical
860 Computing, Vienna, Austria. URL <http://www.R-project.org/>.
861 Razouls C., de Bovée F., Kouwenberg J. et Desreumaux N., 2005-2016. - Diversity and Geographic Distribution
862 of Marine Planktonic Copepods. Available at <http://copepodes.obs-banyuls.fr/en>
863 Reygondeau, G. and Beaugrand, G. 2011. Future climate-driven shifts in distribution of *Calanus finmarchicus*. —
864 *Global Change Biology* 17: 756-766.
865 Richardson, A. J. 2008. In hot water: zooplankton and climate change. — *ICES Journal of Marine Science:*
866 *Journal du Conseil* 65: 279-295.
867 Ridgeway, G. 1999. The state of boosting. — *Computing Science and Statistics* 172-181.
868 Robinson, L. et al. 2011. Pushing the limits in marine species distribution modelling: lessons from the land present
869 challenges and opportunities. — *Global Ecology and Biogeography* 20: 789-802.
870 Rocchini, D. et al. 2011. Accounting for uncertainty when mapping species distributions: the need for maps of
871 ignorance. — *Progress in Physical Geography* 35: 211-226.
872 Roe, H. 1974. Observations on the diurnal vertical migrations of an oceanic animal community. — *Marine Biology*
873 28: 99-113.
874 Roubicek, A. et al. 2010. Does the choice of climate baseline matter in ecological niche modelling? — *Ecological*
875 *Modelling* 221: 2280-2286.
876 Sabatès, A. et al. 2006. Sea warming and fish distribution: the case of the small pelagic fish, *Sardinella aurita*, in
877 the western Mediterranean. — *Global Change Biology* 12: 2209-2219.
878 Sabine, C. L. et al. 2004. The oceanic sink for anthropogenic CO₂. — *science* 305: 367-371.
879 Scotto di Carlo, B. et al. 1984. Vertical zonation patterns for Mediterranean copepods from the surface to 3000 m
880 at a fixed station in the Tyrrhenian Sea. — *Journal of Plankton Research* 6: 1031-1056.
881 Segurado, P. and Araújo, M. B. 2004. An evaluation of methods for modelling species distributions. — *Journal of*
882 *Biogeography* 31: 1555-1568.
883 Sillero, N. 2011. What does ecological modelling model? A proposed classification of ecological niche models
884 based on their underlying methods. — *Ecological Modelling* 222: 1343-1346.
885 Siokou-Frangou, I. et al. 2010. Plankton in the open Mediterranean Sea: a review. — *Biogeosciences* 7: 1543-
886 1586.
887 Soberón, J. and Nakamura, M. 2009. Niches and distributional areas: concepts, methods, and assumptions. —
888 *Proceedings of the National Academy of Sciences* 106: 19644-19650.
889 Stergiou, K. I. and Karpouzi, V. S. 2002. Feeding habits and trophic levels of Mediterranean fish. — *Reviews in*
890 *fish biology and fisheries* 11: 217-254.
891 Sunday, J. M. et al. 2011. Global analysis of thermal tolerance and latitude in ectotherms. — *Proceedings of the*
892 *Royal Society B: Biological Sciences* 278: 1823-1830.
893 Sunday, J. M. et al. 2012. Thermal tolerance and the global redistribution of animals. — *Nature Climate Change*
894 2: 686-690.
895 The MerMex Group. 2011. Marine ecosystems' responses to climatic and anthropogenic forcings in the
896 Mediterranean. — *Progress in Oceanography* 91: 97-166.
897 Thuiller, W. et al. 2004. Effects of restricting environmental range of data to project current and future species
898 distributions. — *Ecography* 27: 165-172.
899 Thuiller, W. et al. 2011. Consequences of climate change on the tree of life in Europe. — *Nature* 470: 531-534.
900 Thuiller, W. et al. 2013. biomod2: Ensemble platform for species distribution modeling. — R package version 2:
901 r560.
902 Thuiller, W. et al. 2015. From species distributions to meta- communities. — *Ecology Letters* 18: 1321-1328.
903 Tsoar, A. et al. 2007. A comparative evaluation of presence-only methods for modelling species distribution. —
904 *Diversity and distributions* 13: 397-405.
905 Villarino, E. et al. 2015. Modelling the future biogeography of North Atlantic zooplankton communities in response
906 to climate change. — *Mar Ecol Prog Ser* 531: 121-142.
907 Yackulic, C. B. et al. 2013. Presence- only modelling using MAXENT: when can we trust the inferences? —
908 *Methods in Ecology and Evolution* 4: 236-243.
909 Zimmermann, N. E. et al. 2010. New trends in species distribution modelling. — *Ecography* 33: 985-989.
910 Zurell, D. et al. 2012. Predicting to new environments: tools for visualizing model behaviour and impacts on
911 mapped distributions. — *Diversity and Distributions* 18: 628-634.
912 Zweng, M. et al. 2013. World Ocean Atlas 2013. Vol. 2: Salinity. — NOAA Atlas NESDIS 74: 39.

913 Supplementary material (Appendix EXXXXX at <www.oikosoffice.lu.se/appendix>).
914 Appendix 1–2.

915

916 **Figure captions**

917

918 **Fig. 1)** Schematic summary of the analytical framework of the study. For each 106
919 species, environmental weighting and spatial buffering are used to generate 10
920 P/psA datasets and each is used to calibrate 10 different ENMs. The niche models
921 are used to project species habitat suitabilities in present (1965-1994) and future
922 (2020-2049; 2069-2098) time periods at the regional scale. Different configurations
923 (SRES and BF) of the regional circulation model are used to investigate their relative
924 contribution to uncertainties. Habitat suitability maps are transformed into binary
925 (P/A) maps (maximizing TSS threshold criterion) which are used to generate the
926 species assemblages. Differences in species richness (Δ SR) and composition (β div
927 indices) are computed by comparing the assemblages of 2020-2049 and 2068-2098
928 to the 1965-1994 assemblages.

929

930 **Fig. 2)** Changes in species richness and composition between the baseline period
931 (1965-1994) and 2020-2049 (a,c) and 2069-2098 (b,d) for the copepod assemblages
932 of the surface Mediterranean Sea. Changes in species composition are quantified
933 using Jaccard's dissimilarity index β_{jac} (a,b) and the β ratio index (c,d). Numbers in
934 (d) indicate the main Mediterranean sub-basins: 1) Alboran Sea 2) Algerian and
935 Tunisian waters 3) Gulf of Lions 4) Ligurian Sea 5) Tyrrhenian Sea 6) Sicilian Strait
936 7) Tunisian and Libyan shelf waters 8) Ionian Sea 9) Adriatic Sea 10) Levantine Sea
937 11) Aegean Sea.

938

939 **Fig. 3)** Linear relationships between the average value of predicted Δ SR and the
940 associated standard deviation, for the Mediterranean cells exhibiting both losses and
941 increases in richness. Mean Δ SR values come from all ENMs predictions for the
942 2069-2098 period. The two linear model statistics are given in the figure.

943

944 **Fig. 4)** Proportion of the total sum of square attributed to the following source of
945 uncertainties: (a) ENM, GHG emission scenario (SRES), species prevalence, and
946 associated interaction terms, and (b) ENM, boundary forcings, species prevalence
947 and associated interaction terms, for the two future time periods (2020-2049;
948 2069-2098).

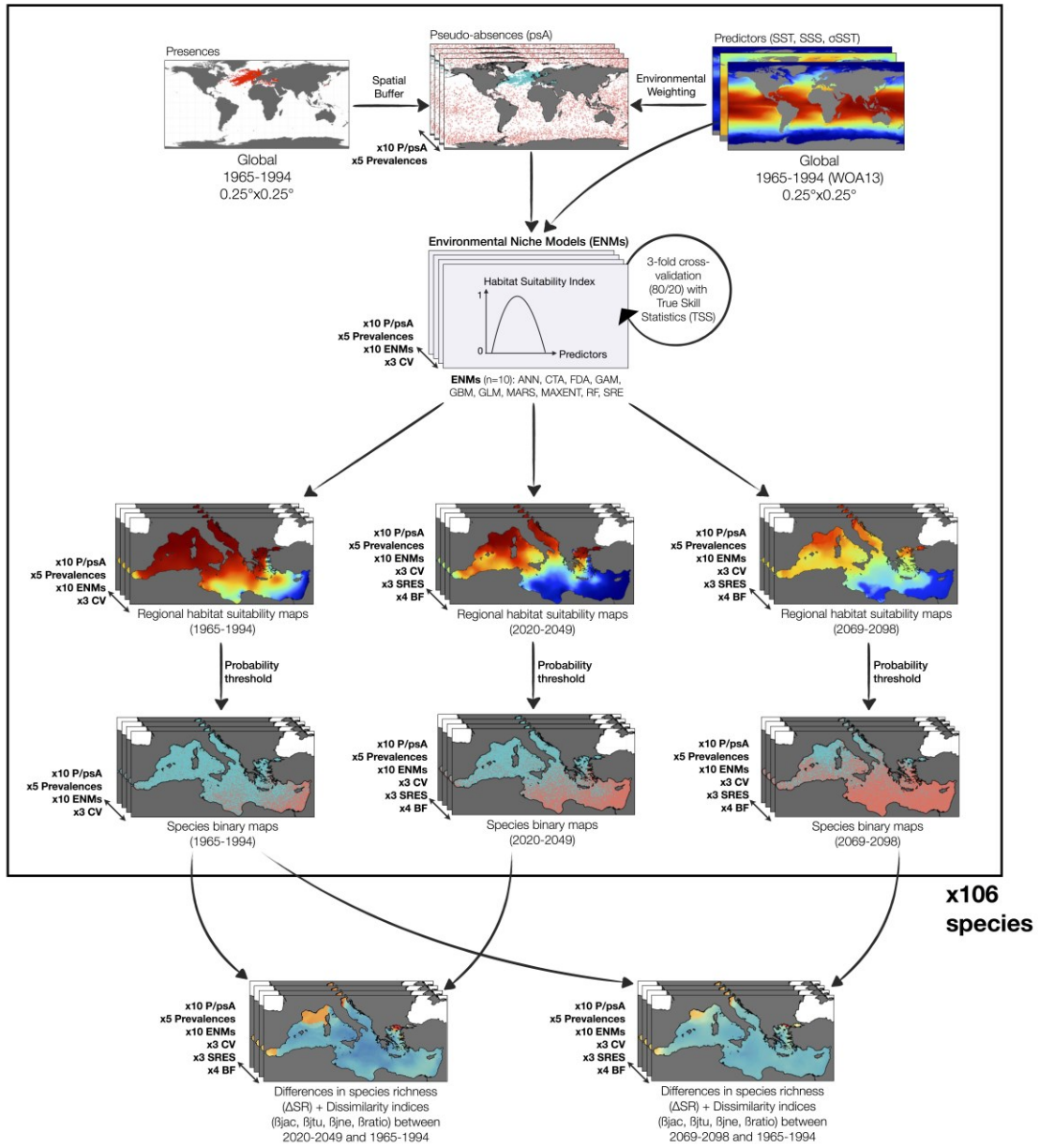
949

950 **Fig. 5)** (a) Relative contribution of the 10 ENMs to the first two Principal Components
951 of a PCA, SRE projections are incomparable to presence-absence and presence-
952 background ENMs' forecasts. (b) Consensus changes in species richness and
953 surface assemblages composition between the baseline (1965–1994) and the future
954 (2069–2098) time periods, based on SRE models only, quantified using the Jaccard's
955 dissimilarity index β_{jac} .

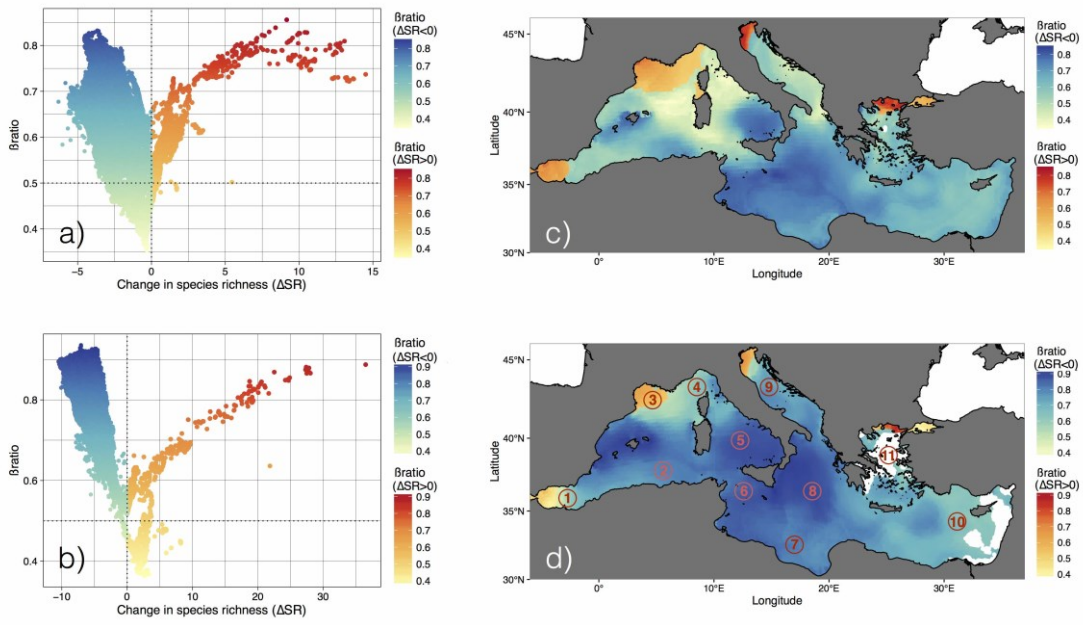
956

957 **Fig. 6)** ENMs loadings (excluding SRE) on the first Principal Component (72.36% of
958 explained variance) of an un-scaled PCA based on their mean projections of Δ SR for
959 the 2069-2098 period. Colors and shapes describe the forcing configuration of the
960 circulation model (BF and SRES). PC1 represents a gradient in predicted species
961 losses (negative Δ SR), ENMs with higher loadings are the ones predicting greater

962 rates of species loss. Within-ENM spreading of the loadings along PC1 indicates the
963 method sensitivity to the choices of the SRES/BF (i.e. the strength of interactions).
964
965
966
967

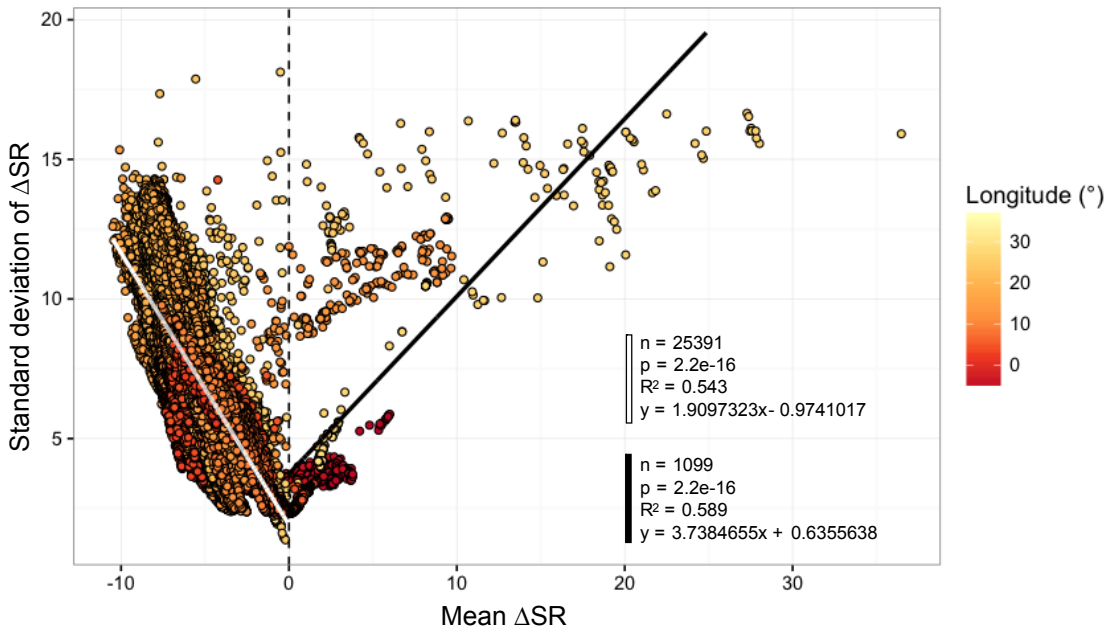


972 **Figure 2**



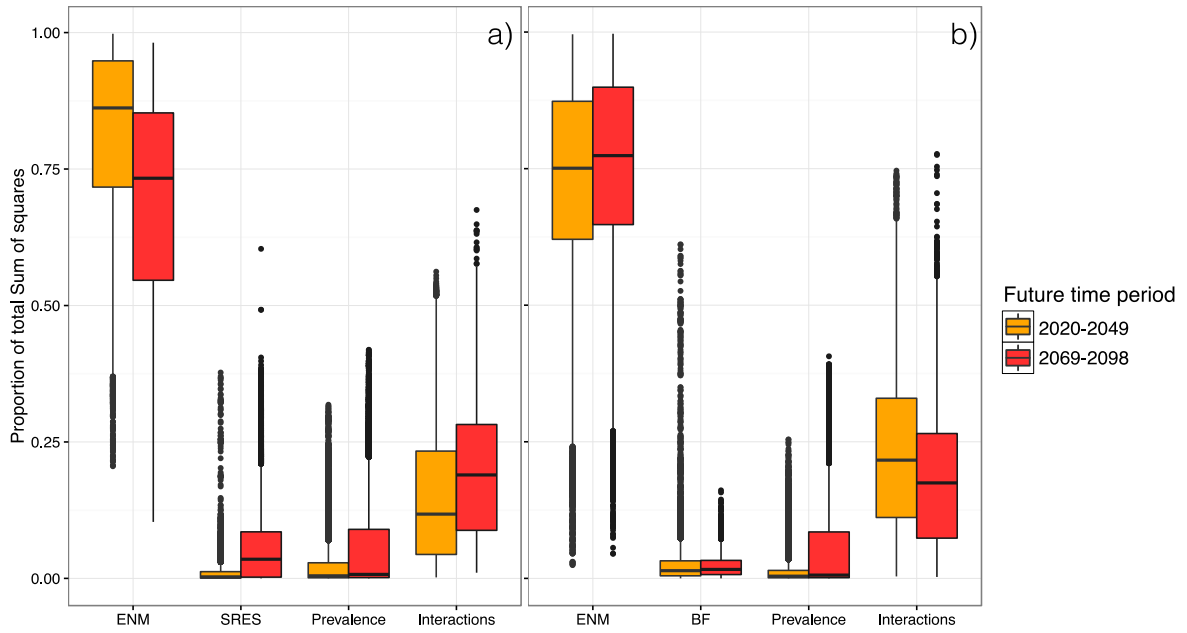
973
974
975
976
977
978

Figure 3



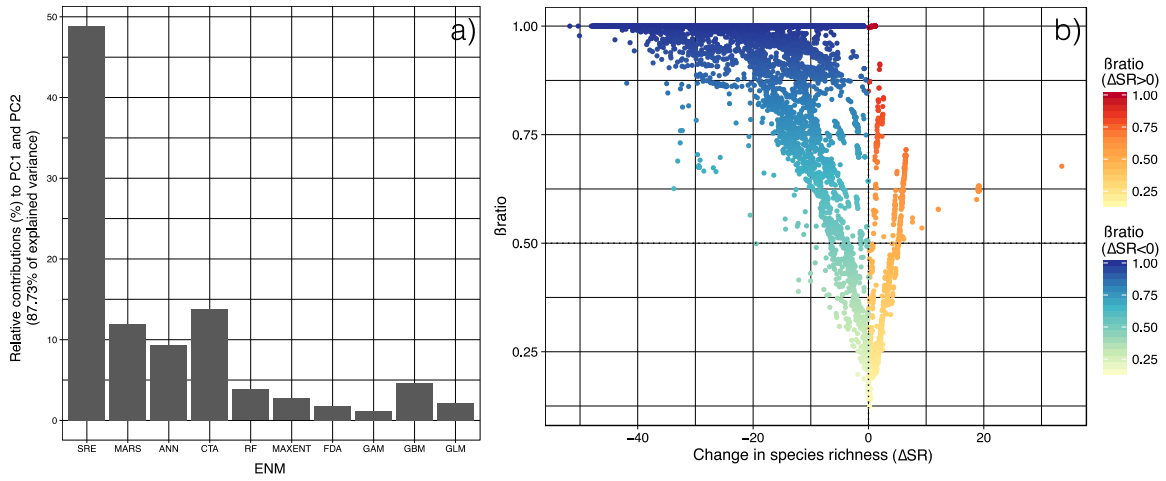
979
980

981 **Figure 4**



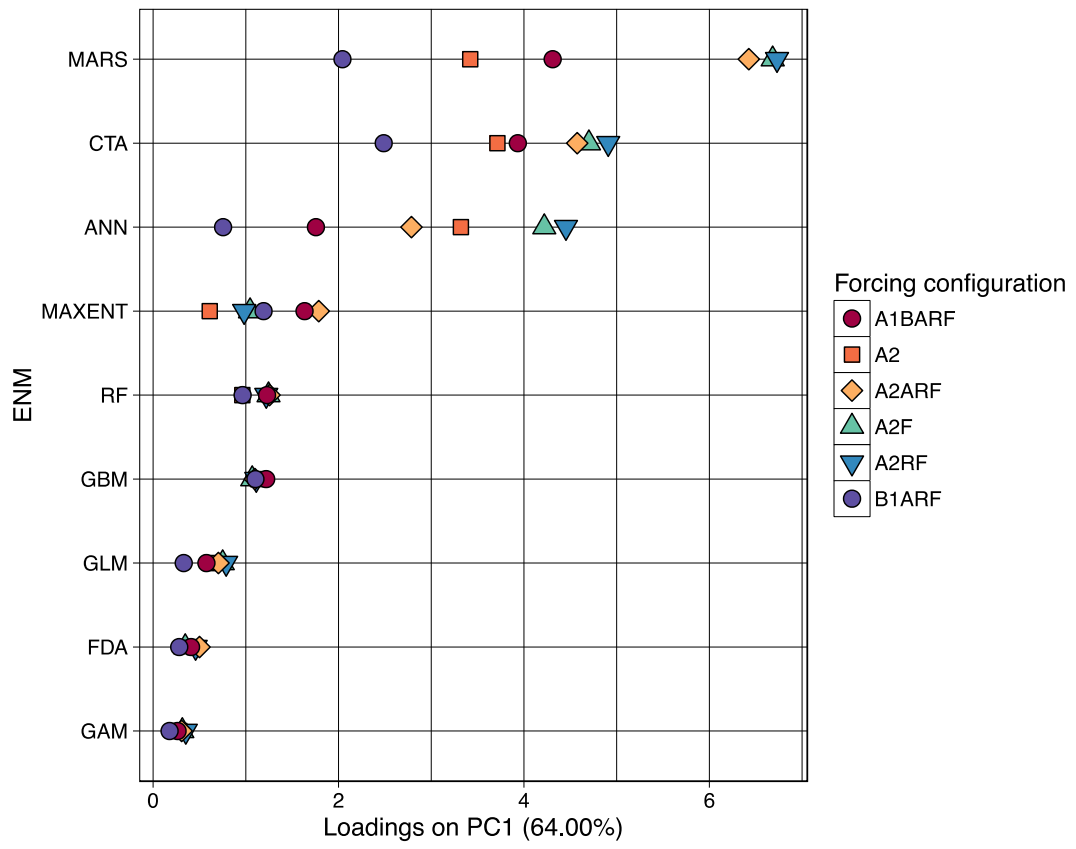
982
983
984
985
986
987
988

Figure 5



989
990
991
992
993

994 **Figure 6**
995



996
997

998 **Supplementary material Appendix**

999

1000 **Supplementary Table A1** - References used to build the copepod species list, with
1001 the associated number of occurrences, the covered subregion of the Mediterranean
1002 Sea and the time period encompassing the occurrences.

1003

1004 **Supplementary Table A2** - Copepod species list and corresponding numbers of
1005 global, and regional, presence cells (after re-sampling on WOA13's grid, 0.25x0.25°
1006 resolution).

1007

1008 **Supplementary Table A3** - Summary of the regional ocean circulation model
1009 (NEMOMED8) outputs in terms of SST, σ SST and SSS for each of its configurations
1010 (i.e. combination of SRES and BF). Differences against WOA13 climatologies and
1011 modelled anomalies are also given.

1012

1013 **Supplementary Figure A4** - Species average TSS scores (plus the associated
1014 confidence intervals). ENMs were cross-validated by dividing each P/psA dataset into
1015 a training set (80% of the data) and a testing set (remaining 20%).

1016

1017 **Supplementary Figure A5** - ENMs average TSS (plus the associated confidence
1018 intervals). ENMs were cross-validated by dividing each P/psA dataset into a training
1019 set (80% of the data) and a testing set (remaining 20%).

1020

1021 **Supplementary material Appendix, Tables captions**

1022

1023 **Table A1)** References used to build the regional occurrence database and the
1024 copepod species names list. The associated number of occurrences, the covered
1025 subregion of the Mediterranean Sea, and the time period covering the occurrences
1026 are given.

1027

1028 **Table A2)** Copepod species list and corresponding numbers of global, and regional,
1029 presence cells (0.25x0.25° resolution).

1030 The species names list was obtained as follows: several regional (i.e. Mediterranean)
1031 datasets were merged (see Suppl. Table S1) to build a regional occurrence database
1032 which recorded 361 different species; then, only the species with at least 50 different
1033 records (meaning at least 50 different observation points in time and space) were
1034 kept in order to get rid of species rarely occurring in the basin of interest (n=193);
1035 finally, in order to avoid truncated response curves (Thuiller et al. 2004) as all
1036 species are not proven endemic to the Mediterranean Sea (Razouls et al. 2005-
1037 2016), the species name list was further restricted to species presenting several
1038 occurrences in other oceanic basins on the OBIS online database (assessed on the
1039 11 December 2014). It consists of the species that are the most commonly sampled
1040 in the surface (0-300m depth) of the Mediterranean Sea (Siokou-Frangou et al. 2010;
1041 Mazzocchi et al. 2014; Benedetti et al. 2016).

1042 The occurrences of the final 106 chosen species were re-sampled on the WOA13
1043 grid cell (0.25x0.25° resolution; Levitus et al. 2013). The final number of global, and
1044 regional, grid cells with presences are given here. In the regional database, species
1045 can present several occurrences belonging to a single 0.25x0.25° cell (because of
1046 records that are spatially close), so that their final number of regional presence cells
1047 is less than 50.

1048
1049 **Table A3)** Summary of the regional ocean circulation model (NEMOMED8) outputs
1050 in terms of SST, σ SST and SSS for each of its configurations (i.e. combination of
1051 SRES and BF). Differences against WOA13 climatologies and modelled anomalies
1052 are also given.

1053 For the baseline period (1965-1994), average values of SST, σ SST and SSS come
1054 from WOA13 climatologies and the two historical configurations of NEMOMED8 (HIF
1055 and HIS-F, see Adloff et al. 2015 for full details). Mean differences between
1056 NEMOMED8 and WOA13 outputs are shown. For the two future time periods (2020-
1057 2049; 2069-2098), mean values are computed on the final climatologies (i.e. the
1058 ones used to project the ENMs) that result from the addition of NEMOMED8
1059 anomalies (as shown in the table) on WOA13 climatologies. Said anomalies were
1060 computed by subtracting historical climatologies (based on HIS runs for the A2
1061 configuration, and HIS-F for all the others, Adloff et al. 2015) to the climatological
1062 future runs.

1063
1064 **Figure A4)** Frequency distribution of the species' average TSS scores, per bins of
1065 0.01 TSS values. The scores were computed with the maximum-threshold method.
1066 ENMs were cross-validated by dividing each P/psA dataset into a training set (80% of
1067 the data) and a testing set (remaining 20%).

1068
1069 **Figure A5)** ENMs' average TSS scores (plus associated standard deviations),
1070 computed with the maximum-threshold method. ENMs were cross-validated by
1071 dividing each P/psA dataset into a training set (80% of the data) and a testing set
1072 (remaining 20%).

1073
1074 **References used in the Supplementary materials' captions:**

- 1075 Adloff, F. et al. 2015. Mediterranean Sea response to climate change in an ensemble of twenty first century
1076 scenarios. — *Climate Dynamics* 1-28.
1077 Benedetti, F. et al. 2016. Identifying copepod functional groups from species functional traits. — *Journal of*
1078 *Plankton Research* 38: 159-166.
1079 Levitus, S. et al. 2013. The World Ocean Database. — *Data Science Journal* 12: WDS229-WDS234.
1080 Mazzocchi, M. et al. 2014. Regional and seasonal characteristics of epipelagic mesozooplankton in the
1081 Mediterranean Sea based on an artificial neural network analysis. — *Journal of Marine Systems* 135: 64-80.
1082 Meynard, C. N. and Kaplan, D. M. 2013. Using virtual species to study species distributions and model
1083 performance. — *Journal of Biogeography* 40: 1-8.
1084 Razouls C., de Bovée F., Kouwenberg J. et Desreumaux N., 2005-2016. - Diversity and Geographic Distribution
1085 of Marine Planktonic Copepods. Available at <http://copepodes.obs-banyuls.fr/en>
1086 Siokou-Frangou, I. et al. 2010. Plankton in the open Mediterranean Sea: a review. — *Biogeosciences* 7: 1543-
1087 1586.
1088 Thuiller, W. et al. 2004. Effects of restricting environmental range of data to project current and future species
1089 distributions. — *Ecography* 27: 165-172.